IOPscience iopscience.iop.org

Home Search Collections Journals About Contact us My IOPscience

Investigation of the electronic properties of strained ZnSe/ZnTe(001) superlattices

This article has been downloaded from IOPscience. Please scroll down to see the full text article.

2003 J. Phys.: Condens. Matter 15 6513

(http://iopscience.iop.org/0953-8984/15/38/018)

View the table of contents for this issue, or go to the journal homepage for more

Download details:
IP Address: 171.66.16.125
The article was downloaded on 19/05/2010 at 15:14

Please note that terms and conditions apply.

INSTITUTE OF PHYSICS PUBLISHING JOURNAL OF PHYSICS: CONDENSED MATTER

J. Phys.: Condens. Matter **15** (2003) 6513–6525 PII: S0953-8984(03)65549-9

# Investigation of the electronic properties of strained ZnSe/ZnTe(001) superlattices

**Nacir Tit**

Physics Department, UAE University, PO Box 17551, Al-Ain, United Arab Emirates

E-mail: ntit@uaeu.ac.ae

Received 1 July 2003
Published 12 September 2003
Online at stacks.iop.org/JPhysCM/15/6513

**Abstract**
The empirical $sp^3s^*$ tight-binding method, which includes both spin–orbit coupling and strain effects, is employed to investigate the electronic properties of the strained ZnSe/ZnTe(001) superlattices (SLs) versus the biaxial strain, layer thicknesses and valence band offset (VBO). The results show that the conduction-band edge state is always represented by an electron localized within the ZnSe slabs; whereas the valence-band edge state (which is mostly a heavy hole (HH) related to ZnTe) can be controlled by the biaxial strain. In this respect, the results show the existence of a certain critical VBO ($V_c \simeq 0.44$ eV) separating two kinds of hole-confinement character (i.e. for VBO $> V_c$, the HH gets localized within the ZnTe layers and the SL is of type-II; whereas for VBO $\leqslant V_c$, the HH has a tendency to localize at the hetero-interface and, as a consequence, the radiative efficiency is enhanced). Finally, our results are compared to some available photoluminescence data and conclusions about the structural and optical qualities of the experimental samples are drawn.

## 1. Introduction

Over the last two decades, semiconductor physics has developed towards studies of low-dimensional systems which have been possible to synthesize due to the advent of modern growth techniques, such as molecular-beam epitaxy (MBE). Yet II–VI compound semiconductors have not undergone as many investigations as those devoted to III–V compounds, for which numerous applications have been realized, and have long seemed prone to remain embryonic. However, the recent achievement of p-type doping of ZnSe by MBE, followed by the realization of II–VI based blue-light emitters [1] has revived the interest in II–VI compounds. Moreover, the constant progress in epitaxial crystal-growth techniques has allowed the elaboration of heterostructures, which include lattice-mismatched materials. The interfacial biaxial strain has been explored in tuning properties suitable for device applications. Among good candidates for the realization of blue-light emitters, strained

 © 2003 IOP Publishing Ltd Printed in the UK 

ZnSe/ZnTe superlattices (SLs) have been interesting structures to tune wavelengths by the variation of the layer thicknesses [1].

As a matter of fact, both ZnSe and ZnTe are promising candidates for optoelectronic materials because they have direct band gaps lying within the visible-light spectrum. The ZnSe/ZnTe strained-layer SLs have been proposed as a means of providing both p- and n-type materials through the modulation doping method, especially for use as hole injection layers in a p–n junction diode giving blue-light emission [1–4]. Such SLs may also present efficient non-linear optical behaviour (optical bistability has been observed [2]). All these properties make such SLs strong candidates in the area of wide gap semiconductors. The main characteristics of ZnSe/ZnTe SLs can be summarized as follows:

(i) The existence of a large mismatch of about 7.2% between the two host materials. Of course, caution has to be exercised, because when the layer thickness exceeds a certain critical value (of about 2 nm), the strain distribution is deeply modified by creation of defects and misfit dislocations in the neighbourhood of the interface. The final state depends on the structure and is not always well known. As a matter of fact, knowing the strain distribution in highly strained SLs is on its own a rather complex problem, and shall be addressed in the present investigation.

(ii) The optical properties show evidences of a type-II band structure, where electrons are confined in ZnSe layers while holes are confined in ZnTe layers.

The spatial indirect transition of separately confined electrons and holes is very weak and therefore difficult to observe in photoluminescence (PL) measurements. The above two characteristics make it obvious to favour the design of thin-layer SLs in order to avoid structural defects and obtain efficient emissions so that the optical quality is the best possible [1–4].

The strong green–blue photoemissions observed in such type-II heterostructures are attractive and deserve theoretical investigations for their interpretation. Some authors [5, 6] have argued that the image charge effects, correlated to the difference in dielectric constants between ZnSe and ZnTe, play an important role in the localization of electrons and holes at the interfaces. Moreover, in another related work on $ZnTe_xSe_{1-x}$ alloys [7–9], it has been demonstrated that Te atoms in a ZnSe host crystal act as isoelectronic traps, and that the emission efficiency of excitons captured at the traps is very high. The wavelength of the PL emission due to these traps depends on the density of Te in ZnSe. The emission light is *blue* for low Te density (namely, $ZnSe_{0.995}Te_{0.005}$) [8] and *green* for relatively higher density (namely, $ZnSe_{0.95}Te_{0.05}$) [9] alloys. The origin of blue emission is due to the Te atom traps in ZnSe. The emission colour is green when the Te atoms form larger clusters. On the other hand, in the case of SLs, the green emission was achieved at room temperature for superstructures having one nominal layer of ZnTe [3]. We emphasize here that the reason for this emission, as well as the effect of layer thicknesses, is within the scope of our present investigation.

On the experimental side, the first successful growth of ZnSe/ZnTe SLs was reported by Kobayashi and co-workers [10]. We emphasize that the atomic-layer epitaxy (ALE) [11] is interesting as a suitable growth technique for the fabrication of such SLs, and is particularly suitable for growing SLs consisting of very thin layers with large strain. To date, these SLs have been grown by growth techniques of various sophistication such as MBE [10, 12–14], ALE [15, 16], hot-wall epitaxy (HWE) [17, 18] and metal–organic vapour-phase epitaxy (MOVPE) [2]. The optical properties of these SLs were first reported by Kobayashi *et al* [10] and Kuwabara *et al* [17], where strong PL spectra were obtained by both groups. The structural and optical properties of these SLs have been examined by x-ray diffraction, transmission electron microscopy (TEM) and Raman scattering techniques [19, 20].

On the theoretical side, it is well established that common-anion III–V [21] as well as II–VI [22–24] heterojunctions have vanishing or small valence band offset (VBOs). As a result, it is legitimate to suspect that the common-cation heterojunctions may be characterized by a vanishing conduction band offset (CBO), as in the case of ZnS/ZnSe SLs [25, 26]. However, it turns out that this is not always true; for instance in the present case of ZnSe/ZnTe SLs the CBO can be as large as the VBO. This latter varies from 0.36 to 1.4 eV depending on the strain state. In regard to the determination of band offsets for ZnSe/ZnTe SLs, we emphasize that despite extensive experimental and theoretical investigations, the value of the VBO is still not well known. The reported results are scattered, as indicated by the previous broad range of values. The experimental VBO results available for ZnSe/ZnTe are sometimes contradictory. This may be due to the fact that most of the works are based on indirect determinations such as PL measurements. In this kind of experiment, the determination is usually achieved by varying the VBO in order to fit theoretical results with the first excitonic transition. The suggested VBO value in such fittings is usually near 1.0 eV, in agreement with the electronic affinity difference. For instance, the VBO determined by fitting $\vec{k} \cdot \vec{p}$ results to PL data [10, 17] is 0.975 eV, and the one by fitting to the results of the semi-empirical tight-binding (TB) method [27] is 1.136 eV. Several more theoretical techniques of various sophistication have been attempted to determine the band offsets. The empirical $sp^3s^*$ TB method [28], which includes both spin–orbit coupling and strain effects, yielded 1.02 eV as the unstrained VBO value. Priester *et al* [22] employed the self-consistent tight-binding (SCTB) method and estimated VBO $\simeq$ 1.4 eV for all the stain cases. Recently, however, Qteish *et al* [29] used a very sophisticated method based on the state-of-the-art *ab initio* technique. This latter technique is based on the self-consistent pseudopotential plane wave technique, where the semicore d-electrons were treated as valence states and the results obtained for the VBO were in excellent agreement with PL data [29]. Their published results for the VBO, when the 3d electrons of Zn are included as relaxed states, for interfaces strained to the $ZnSe_xTe_{1-x}$ substrate, can be described as follows: VBO $= 0.54$, 0.82, and 1.14 eV corresponding to $x = 0$, 0.5, and 1 respectively. In the present work, these VBO values are going to be used and will be shown to be physically reliable.

Last, but not least, as far as the electronic band structure calculation is concerned, several computational techniques were limited either by the system size and applicability only to the ground state properties, as in first principle methods, or by complete neglect of the band mixing effects, as in the effective-mass approach (based on the Kronig–Penney model) or in the Hückel method. To overcome such difficulties, we have chosen the $sp^3s^*$ TB method which includes spin–orbit coupling, that in turn is crucially important in the case of II–VI materials [24]. The TB method has proven its reliability for successfully simulating the experimental data while incorporating the microscopic description of the material, where the point group symmetry of the system is included. Within the Slater–Koster scheme [30], the TB method uses a small basis set of atomic orbitals and this gives the method the ability to deal with large systems; it also takes into account the band-mixing effects which are essential in the band structures of systems like quantum dots, wires, SLs and quantum wells. Moreover, confinement and band-mixing effects may compete with strain effects so that all these factors directly affect the band offsets and particularly the carrier confinement character. Hence, for fundamental research, the ZnSe/ZnTe SLs should be good candidates for following the evolution of the electronic structure of type-II heterostructures as a function of the SL layer thicknesses, band offsets and strain configuration.

Furthermore, we emphasize that several computational works [21–29] have been devoted to the calculation of the VBO. Here, in this present investigation, our task is different. We adopt the same formalism as in [24], namely incorporating the strain within the $sp^3s^*$ TB scheme in the presence of spin–orbit coupling. The biaxial strain is treated as a perturbation *posteriorly*

**Table 1.** The empirical $sp^3s^*$ TB parameters, with the inclusion of spin–orbit coupling, for ZnSe and ZnTe in units of electronvolt. The same notation as in [34] is used. The lattice constants ($a_o$) are in ångström units.

| Compound | $a_o$ | $E_s^a$ | $E_p^a$ | $E_s^c$ | $E_p^c$ | $4V_{ss}$ | $4V_{xx}$ | $4V_{xy}$ |
|---|---|---|---|---|---|---|---|---|
| ZnSe | 5.65 | −12.427 | 1.782 | 0.047 | 5.520 | −6.502 | 3.309 | 5.412 |
| ZnTe | 6.08 | −9.190 | 0.627 | −1.420 | 3.779 | −6.642 | 1.940 | 4.077 |
| Compound | $4V_{sp}^{ac}$ | $4V_{ps}^{ac}$ | $E_{s^*}^a$ | $E_{s^*}^c$ | $4V_{s^*p}^{ac}$ | $4V_{ps^*}^{ac}$ | $\lambda_a$ | $\lambda_c$ |
| ZnSe | 1.137 | −5.802 | 7.850 | 8.520 | 1.870 | −3.266 | 0.194 | 0.019 |
| ZnTe | 5.925 | −4.673 | 6.227 | 6.779 | 3.827 | −2.962 | 0.362 | 0.027 |

added to the Hamiltonian. We calculate the band structures of the ZnSe/ZnTe(001) SLs versus the biaxial strain, layer thicknesses and VBO.

This paper is organized as follows. Section 2 gives a brief description of the TB method. Section 3 gives a detailed description and discussion of our obtained results. Special emphasis is given to the carrier confinement behaviour and the characterization of the SL type. Our results are also compared to some available PL experiments. The final section summarizes our main conclusions.

## 2. Computational details

The parametrized TB method has been successfully used in several areas of solid state physics for many years [31–35]. The inclusion of both spin–orbit interaction and strain effects has, in particular, made the method more attractive for II–VI materials. For the details of this technique, we refer the reader to [26]. However, in our present investigation, we emphasize that we use improved empirical TB parameters [34], which have been proven to successfully reproduce the photoemission and reflectivity experiments. These TB parameters are shown in table 1. Moreover, in the SL calculations, we mention that the validity of two main points is assumed: (i) the macroscopic theory of elasticity (MTE) [36] in evaluating the SL atomic structure, and (ii) the problem of energy reference between the two constituents is resolved by taking the VBO into account [24]. (For instance, in the present case, ZnTe on-site energies are shifted up by the VBO since the valence-band (VB) edge of this constituent is always higher in energy than that of ZnSe when the interface is formed between both of them.) Hence, the VBO is also assumed to simulate all various interface specific effects.

## 3. Results and discussion

### *3.1. FCC bulk bandstructure*

For a bulk semiconductor in a *fcc* structure, the spin–orbit interaction makes the six-fold degenerate states, located at the top of the VB, split into four-fold degenerate states (named spin-degenerate heavy-hole (HH) and light-hole (LH) states) higher in energy, and double-degenerate states (called spin-off 'SO' states) lower in energy. In figure 1, we display the electronic band structures of a bulk *fcc* of both ZnSe (a) and ZnTe (b). These results were obtained using the 10-band ($sp^3s^*$ with inclusion of spin degeneracy) model whose parameters are presented in table 1. In both panels, the VB edge is taken as an energy reference. The respective energy gaps for ZnSe and ZnTe are *direct* and their values are $E_g = 2.82$ and 2.39 eV, which completely agree with the experimental values [36]. The irreducible representations

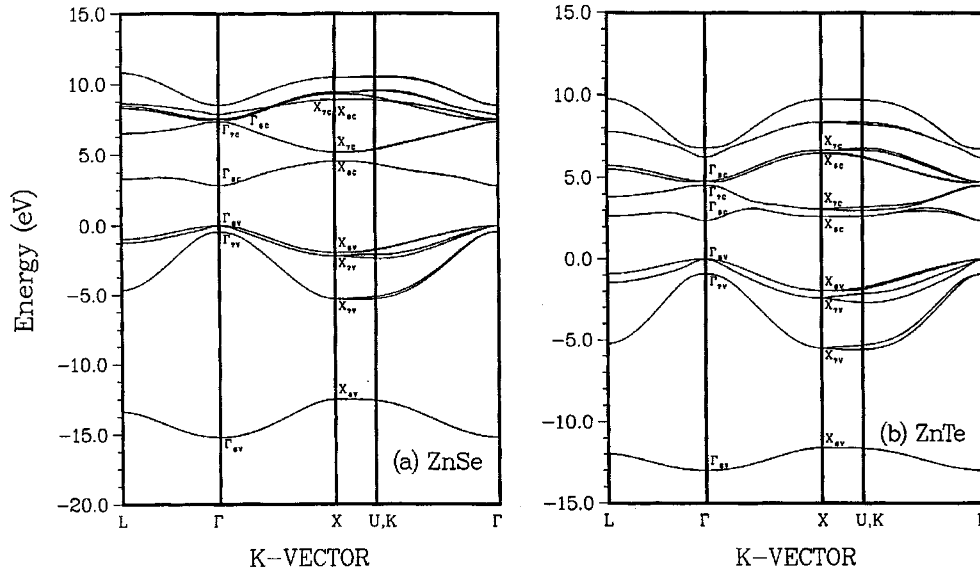


**Figure 1.** The electronic band structures of both (a) *fcc* bulk ZnSe and (b) *fcc* bulk ZnTe, calculated using the $sp^3s^*$ TB model, with the inclusion of spin–orbit coupling. The VB edge is taken as an energy reference.

corresponding to the point group symmetry of the eigenfunctions are also shown in figures 1(a) and (b) for the high-symmetry points Γ and X of the *fcc* Brillouin zone (BZ). In both of these latter panels, the lowest group is dominated by the contribution from the s-orbitals of anion (Se or Te) atoms. The second group, which forms the VB, consists of the cationic s states and all the p states. The third group of bands, which form the conduction band (CB), are mainly due to contributions from the p- and $s^*$-orbitals.

Figure 2 shows the variation of the energy gap ($E_g$) for (i) bulk ZnSe under tensile strain, and (ii) bulk ZnTe under compressive strain. In both of these materials $E_g$ decreases as the in-plane lattice constant $a_\parallel$ increases. More details about the biaxial-strain effects are discussed further in our previous work [24]. In the present work, we emphasize that the VB top state for ZnSe under tensile strain is a LH state; whereas that for ZnTe under compressive strain is a HH state. Moreover, the fact that the $E_g$ of ZnTe is smaller by about 0.15 eV than that of ZnSe and the VBO is no less than 0.36 eV (with the VB edge of ZnTe being higher in energy than that of ZnSe) indicates that the heterostructure is always of type-II. More details about the carrier confinement properties will be discussed below.

### *3.2. Superlattice bandstructure*

Figure 3 displays the energy gap variation of the $(ZnSe)_n(ZnTe)_n(001)$ SLs versus the biaxial strain, VBO and the layer thickness $n$. In mapping the strain effects, we have chosen to work on three differently strained SLs; two of which are extremely strained to either ZnSe (figure 3(a)) or ZnTe (figure 3(c)). The third one is the case of the intermediate strain state, where the SL is strained to the $ZnSe_{0.5}Te_{0.5}$ substrate (figure 3(b)). This latter case is almost similar to a free-standing SL. In all three cases, we have assumed in our calculations that the SLs are *pseudomorphic* (defect free) and that the MTE is valid in evaluating the SL atomic structure. For each panel of figure 3, we have considered two extreme values of VBO to span the existing

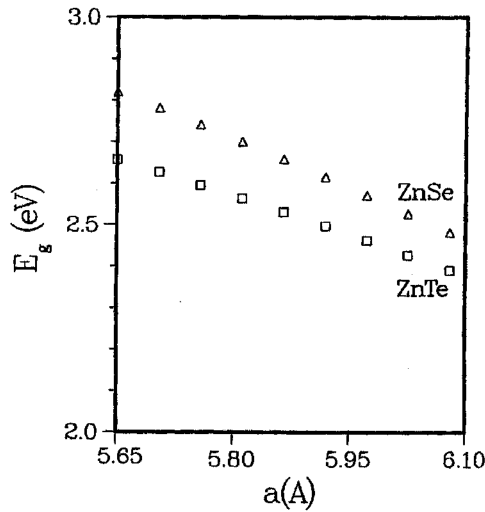


**Figure 2.** The variation of $E_g$ versus the in-plane lattice constant $a_\parallel$. The ZnSe is under *tensile* strain whereas the ZnTe is under *compressive* strain. The VB edge is taken as an energy reference.

range of values in the literature. In figure 3(a), we took as a lower bound VBO = 0.85 eV, which corresponds to the midgap theory of Tersoff [37] and as an upper bound VBO = 1.45 eV, which corresponds to the SCTB of Priester *et al* [22]. In figure 3(b), which corresponds to the $ZnSe_{0.5}Te_{0.5}$ substrate, we took as a lower bound VBO = 0.76 eV, which is due to the work of Qteish *et al* [29] when only the linear deformation potential (LDP) is included, and as an upper bound VBO = 1.43 eV, which is due the SCTB of Priester *et al* [22]. In figure 3(c), which corresponds to the ZnTe substrate, we took as a lower bound VBO = 0.42 eV, which is due to the LDP approach of Qteish *et al* [29], and as an upper bound VBO = 1.41 eV, which is due to the SCTB of Priester *et al* [22]. The variation in the VBO in each of these three panels reflects the scattered estimates found in the literature. Our results for all the studied SLs show that the VB edge always consists of HHs related to ZnTe, but has a localization character sensitive to the substrate (or VBO). We emphasize that the CB edge (electron) is always localized within the ZnSe slabs. We furthermore emphasize that two different symbols are used in figure 3 to indicate the type of the SL character: (i) the symbol $\times$ stands for a SL of type-II, where the HH is completely confined within ZnTe layers, and (ii) the symbol $\otimes$ stands for a SL not well characterized as the HH is delocalized over the whole SL. In figure 3, now, we shall discuss the effects of strain, layer thickness ($n$), and VBO on the SL bandstructure:

(i) The energy gap ($E_g$) decreases as the substrate is modified from ZnSe to ZnTe (i.e. $a_\parallel$ increases) and this trend is also represented in figure 2.

(ii) The $E_g$ decreases with increasing $n$ as an effect of carrier quantum confinements. This reduction is more pronounced when the VBO is large and the SL becomes of stronger type-II character because the confinement of the HH and electron are then independent. In figure 3(c), the curve of VBO = 0.42 eV is almost insensitive to layer thickness $n$ because the HH has a tendency to localize at the interface, as will be shown below.

(iii) The range of VBO values used in both figures 3(a) and (b) always yield a SL of type-II.

The only possibility of having HH delocalized over the whole SL exists only in figure 3(c), whose corresponding substrate is ZnTe. Therefore, a relatively high radiative efficiency is expected for the SLs of figure 3(c) when the VBO is the smallest possible.

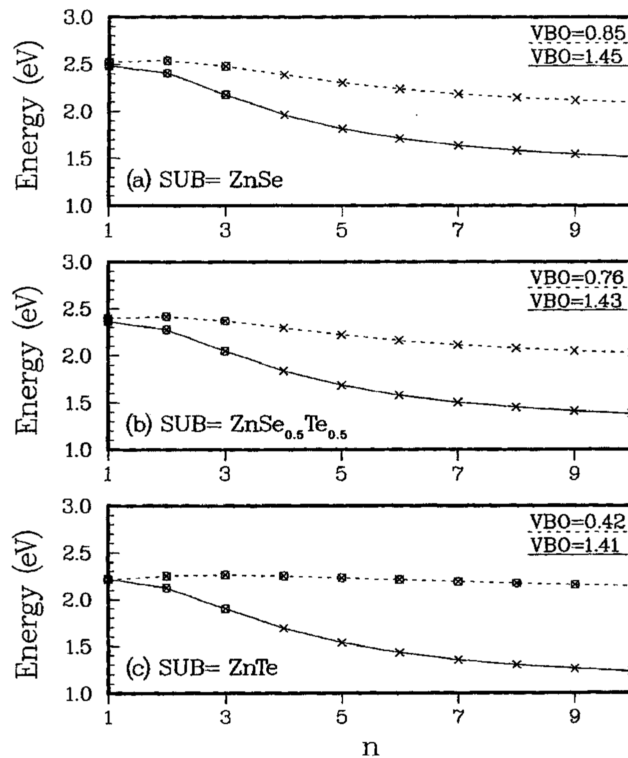


**Figure 3.** The variation of the energy gap of the $(ZnSe)_n(ZnTe)_n(001)$ SL versus $n$. Each panel represents one biaxial strain state. Different values of VBO are considered for each case. The character of the SL is indicated by the symbols (see text for details).

In figure 4, we display the energy gap of the $(ZnSe)_{10}(ZnTe)_{10}(001)$ SL, calculated at $\Gamma$-point, versus VBO for three different substrates: (a) ZnSe; (b) $ZnSe_{0.5}Te_{0.5}$; and (c) ZnTe respectively. The SL–VB edge is taken as an energy reference. In the insets of figure 4, we show the energy difference between the two highest SL–VB states ($E_{v1} - E_{v2}$) versus VBO. One common result between the three insets of figure 4 is that $E_{v1}$ and $E_{v2}$ states get close in energy at $V_c \simeq 0.44$ eV then separates apart thereafter. This striking result in which ($E_{v1} - E_{v2}$) has a minimum value is independent of the strain state (or substrate). As far as our TB scheme is concerned, the results show that if VBO $< V_c$, the HH is delocalized; and if VBO $\simeq V_c$ the HH get localized at the interface; and finally if VBO $> V_c$ the HH get localized with ZnTe slabs. Finally, we mention that the range of VBO used in figure 4 is not realistic but rather mathematical for just to study the behaviour of the hole under the action of VBO variation.

To assess the effect of band offsets on the carrier confinement character, we display in figure 5 the wavefunction-squared amplitudes of two highest hole states ($E_{v1}$ and $E_{v2}$) and one lowest electron state ($E_{c1}$), at $\Gamma$-point, for $(ZnSe)_{10}(ZnTe)_{10}(001)$ SL, grown on a $ZnSe_{0.5}Te_{0.5}$ substrate, versus the spatial growth direction ($c$-direction). Here, the choice of the SLs of the $ZnSe_{0.5}Te_{0.5}$ substrate was made because they yield a strain state very close to the one of a free-standing SL, which could be the case of many grown samples as far as the high lattice mismatch is concerned, and liklihood of the occurrence of misfit dislocations is high. The range of the VBO used is from 0.20 to 0.80 eV, within which the band anticrossing occurs between the VB top states at $\Gamma$-point. Three values of VBO have been chosen:

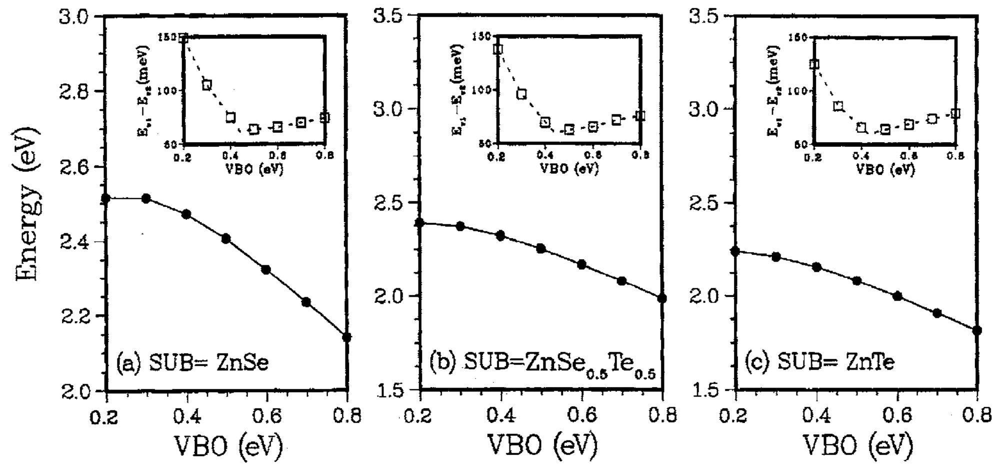


**Figure 4.** The variation of the lowest CB state $E_{c1}$ versus the VBO for three different substrates: (a) ZnSe, (b) $ZnSe_{0.5}Te_{0.5}$ and (c) ZnTe for the $(ZnSe)_{10}(ZnTe)_{10}(001)$ SLs. The SL–VB edge is taken as an energy reference in each case. The inset shows the variation of $(E_{v1} - E_{v2})$ versus the VBO.

(i) In figure 5(a), VBO = 0.20 eV. Of course, the physical VBO is much higher than this value and this is just used as mathematical lower bound in order to clearly demonstrate the crossover of the HH localization behaviour.

(ii) In figure 5(b), VBO = 0.44 eV, which is the critical value predicted by our present work (see figure 4).

(iii) In figure 5(c), VBO = 0.80 eV, which is close to the value published by Qteish *et al* [29], and is used as an upper bound.

For the realistic range of VBO (>0.44 eV), figure 5 shows that the bottom of the SL–CB (electron) state is always localized within the ZnSe slabs (see the $E_{c1}$ state in figures 5(b) and (c)). In contrast, the top of the SL–VB (HH) state has a tendency to localize at the interface for VBO $\leqslant$ 0.44 eV (see the $E_{v1}$ state in figures 5(a) and (b)). As expected, the HH becomes localized within ZnTe slabs when VBO > 0.44 eV as shown in figure 5(c). In figure 5, the second highest VB state ($E_{v2}$) is shown to be localized within ZnTe slabs regardless of the strain state (or VBO). Hence, figure 5 corroborates the idea of the existence of a critical VBO ($V_c \simeq 0.44$ eV), above which the SL behaves as pure type-II. This value is, in fact, independent of the strain state as indicated by figure 4. This result would be very useful for the case of ZnTe substrate, where the VBO is the smallest possible and can be close to $V_c$. Of course, we should mention that figures 4 and 5 are still unable to fully demonstrate the band anticrossing because this requires the presence of interaction effects, which are missing in the TB single-particle picture.

To further elaborate this anticipated band anticrossing, we display in figure 6 the band structures for the same SLs of figure 5, calculated along the Z$\Gamma$ high symmetry line of the BZ. We emphasize that the SL–VB edge is taken as an energy reference and that VBO = $E_v$(ZnTe) − $E_v$(ZnSe), where $E_v$ is the VB-edge energy of the material indicated in brackets in the strained configuration corresponding to the SL structure. In figure 6(a), VBO = 0.20 and CBO = 0.07 eV, which yield in fact a SL not well characterized because the electron's wavefunction is extended over the whole SL and, as a consequence, all the CBs are dispersive. On the other hand, the top VB (hole) states are localized and yield nesting bands for all the eigenstates within the depth of the ZnTe well. In figure 6(b), VBO = 0.44 and CBO = 0.31 eV.

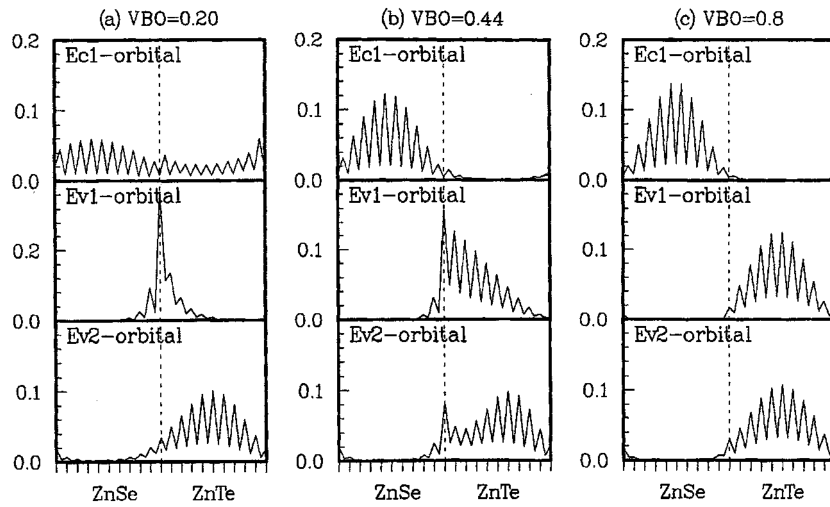


**Figure 5.** The calculated wavefunction-squared amplitudes for the case of $(ZnSe)_{10}(ZnTe)_{10}(001)$ SL, grown on a $ZnSe_{0.5}Te_{0.5}$ substrate, versus the spatial growth (*c*-axis) direction and using: (a) VBO $= 0.20$, (b) VBO $= 0.44$ and (c) VBO $= 0.80$ eV. $E_{c1}$ corresponds to the lowest SL–CB state at the $\Gamma$-point, and $E_{v1}$ and $E_{v2}$ also correspond to the highest SL–VB states at the $\Gamma$-point.

Here, also, the nesting (flat) bands indicate the strong localization of carriers along the growth (*c*-axis) direction. The striking result here is that the VB-edge (HH) state is still localized at the interface (see figure 5(b)) due to both the strong band-mixing effects caused by the biaxial strain and the dielectric-constant difference between the two SL constituents [5, 6]. One can clearly see the strong confinement of electrons in the CB (for instance within about 0.2 eV above the SL–CB edge there are only two spin-degenerate nesting bands or discrete levels in the ZnSe well). On the other hand, within the VBO range below the SL–VB edge, there exist several spin-degenerate nesting bands. Of course, the highest nesting VB, in figure 6(b), correspond to the HH which is localized at the interface as indicated in figure 5(b). In figure 6(c), VBO $= 0.80$ and CBO $= 0.67$ eV. In this case, the carrier wells are very deep to ensure the localization of the HH within ZnTe layers and the localization of electrons within ZnSe slabs. The SL is definitely of pure type-II. Of course, in going from figure 6(a) (not well characterized SL) to figure 6(c) (SL of type-II character), the $E_g$ decreases as a consequence of the fact that in type-II the carriers have stronger confinement characters.

### *3.3. Modelling of photoluminescence experiments*

Since it is difficult to obtain a high-quality single crystal of type II–VI semiconductors, the III–V semiconductors are usually used as a substrate in the growth of II–VI SLs. In the present work, for instance, we consider $(ZnSe)_m(ZnTe)_n(001)$ SLs grown on InAs, InP and GaAs substrates because of the following three reasons: (i) high-quality II–VI compound substrates are not available, (ii) lattice constants of ZnTe, $ZnSe_{0.5}Te_{0.5}$, and ZnSe are very close to those of InAs, InP, and GaAs respectively, and (iii) experimental results are available for comparison.

Figure 7 shows the calculated energy band gaps of $(ZnTe)_m(ZnSe)_{8-m}(001)$ SLs grown coherently on (i) GaAs, (ii) InP and (iii) InAs substrates. In order to allow comparison with the experimental results of [12], $m$ is selected to be between 2 and 6. We mention that the PL data were collected at 71 K and shown in figure 7 by full circles (•). We have theoretically calculated energy gaps ($E_g$) at the $\Gamma$-point for SLs using two different sets of VBO. In each

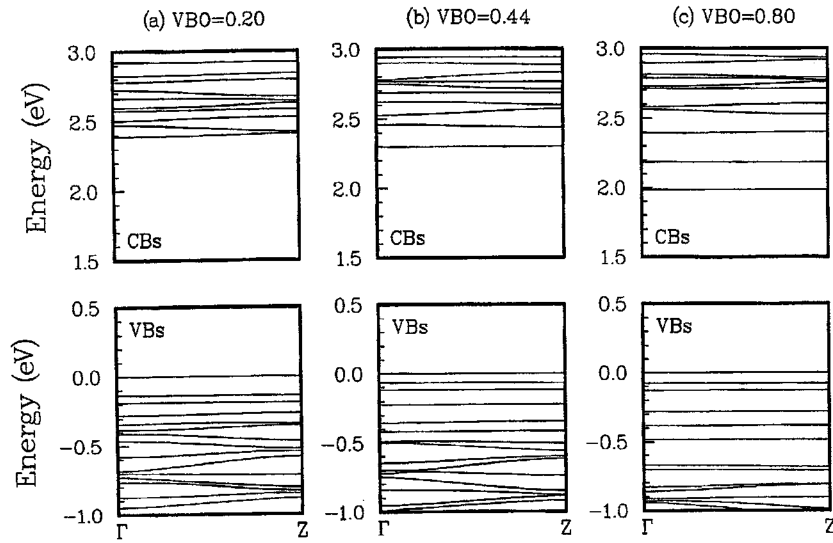


**Figure 6.** The band structures along the ΓZ-symmetry line are displayed for the same SLs of figure 5. The lower parts display the VBs and the upper ones show the CBs. The SL–VB edge is taken as an energy reference.

case in figure 7, the smaller value of VBO corresponds to the *ab initio* calculation of Qteish *et al* [29] and is represented by △ symbols; whereas the larger VBO value corresponds to the MSA of Van de Walle [36] and is represented by □ symbols. According to our above discussion, all the SLs of figure 7 should be of type-II. Both theoretical and experimental data, in figure 7, show some bowing properties similar to the case of $ZnTe_xSe_{1-x}$ alloys. Of course, the bowing parameter seems to be small due to the small $\Delta E_g$ between the two SL constituents. The comparison of our TB results to the PL data, shown in figure 7, yields a relatively poor agreement for the two cases of GaAs and InP substrates (see figures 7(a) and (b)). This disagreement is probably caused by the difficulty in achieving coherent growth of SLs on these latter substrates. A much better agreement, however, is achieved in the case of the InAs substrate (see figure 7(c)). In addition to this latter success in the experimental growth, our theoretical results (discussed above) are also in favour of this particular substrate as it yields the smallest VBO possible, which allows the hole confinement at the interface and, therefore, yields an enhancement in the SL radiative efficiency.

As a matter of fact, the band offsets should remain constant and independent of the slab thicknesses if *pseudomorphic* growth has been achieved. The VBO should depend solely on the biaxial strain (substrate composition). But the occurrence of misfit dislocations is anticipated as far as our present high lattice mismatch (7.2%) is concerned. Because of this latter reason, we emphasize that we found it much easier to use different values of VBO while fitting the PL data, even for samples grown on similar substrates and under the same conditions. The main difference is due to the difference in the strain *morphology* from sample to sample as indicated by the occurrence of misfit dislocations. To solve this problem, we have chosen to study again the SLs of figure 7, but the VBO is adjusted to yield an exact fit of the $E_g$ of the PL data. The results are shown in table 2, which can be summarized as follows:

(i) For samples grown on GaAs substrate, the VBO is varied from 0.70 to 1.95 eV. This huge fluctuation reveals the large difference in the strain *morphology* between the samples and might be an indication of the occurrence of misfit dislocations.

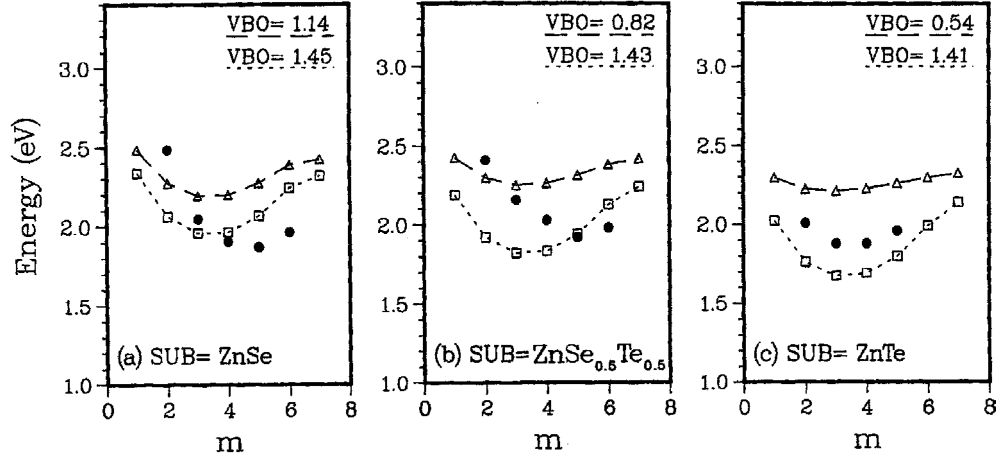


**Figure 7.** Comparison between theoretical results and PL data [12] for $E_g$ of $(ZnTe)_m(ZnSe)_{8-m}(001)$ SLs versus $m$. Symbols ● stand for PL experiments. Theoretical results are shown by △ corresponding to the VBOs of Qteish *et al* [29], and □ corresponding to VBOs of Priester *et al* [22]. The SLs' atomic structures are calculated using the MTE [36].

**Table 2.** The theoretical VBO values, corresponding to the exact fit of the experimental $E_g$ of [12], for the $(ZnTe)_m(ZnSe)_{8-m}(001)$ SLs strained to three different substrates.

| | Substrate = GaAs | | Substrate = InP | | Substrate = InAs | |
|---|---|---|---|---|---|---|
| $m$ | $E_g$ (eV)[a,b] | VBO (eV)[b] | $E_g$ (eV)[a,c] | VBO (eV)[c] | $E_g$ (eV)[a,d] | VBO (eV)[d] |
| 2 | 2.486 | 0.700 | 2.395 | 0.350 | 2.010 | 1.046 |
| 3 | 2.044 | 1.340 | 2.157 | 0.970 | 1.880 | 1.138 |
| 4 | 1.905 | 1.524 | 2.030 | 1.170 | 1.880 | 1.160 |
| 5 | 1.870 | 1.710 | 1.920 | 1.453 | 1.960 | 1.171 |
| 6 | 1.964 | 1.950 | 1.979 | 1.700 | — | — |

[a] PL data due to the work of [12].
[b] Present work using a substrate ZnSe(≡GaAs).
[c] Present work using a substrate $ZnSe_{0.5}Te_{0.5}$(≡InP).
[d] Present work using a substrate ZnTe(≡InAs).

(ii) The same order of VBO fluctuation occurs in the samples grown on an InP substrate and also reflects the difficulty in achieving coherent growth.
(iii) However, for the samples grown on InAs, the VBO is varied from 1.05 to 1.17 eV. This small VBO fluctuation indicates that coherent growth is achieved on InAs substrates. Moreover, these two latter VBO values are consistent with the one estimated by Wu *et al* [27], whose VBO $\simeq$ 1.136 eV.

Last, but not least, good quality free-standing ZnSe/ZnTe SLs have also been successfully grown using low-pressure MOVPE by Cloitre and co-workers [38]. The sample grown was characterized by the x-ray diffraction technique and was found to be a free-standing $(ZnTe)_{14}(ZnSe)_7(001)$ SL and PL measurements were carried out to investigate the optical properties. The electron–HH transition is reported to be at 1.987 eV. We have performed a theoretical fitting and obtained that this value of $E_g$ can be reproduced with VBO = 0.80 eV. This latter value of VBO is consistent with that obtained in the *ab initio* calculation of Qteish *et al* [29]. Thus, we conclude that the sample grown has nearly *pseudomorphic* (good quality) structure and that the theoretical technique used, by Qteish *et al* [29], for VBO determination

is very reliable. From the perspective of our present work, these SLs are of type-II, and PL can be enhanced by using a larger $a_{\parallel}$ buffer, which makes the hole (HH) have a tendency to localize at the interface and this behaviour enhances the radiative efficiency. Of course, as far as the structural quality is concerned, the SL-layer thicknesses must be kept thin enough and the MBE technique is recommended for such a challenging task.

## 4. Conclusions

Within the $sp^3s^*$ TB framework, with inclusion of both spin–orbit coupling and strain effects, the electronic band structures of the strained-layer ZnSe/ZnTe(001) SLs have been investigated versus the biaxial strain, layer thicknesses and VBO. The results show that all these SLs are of type-II, where the VB-edge state is represented by a HH localized within ZnTe slabs and the CB-edge state is represented by an electron always confined in ZnSe layers. Furthermore, our theoretical results show the existence of a critical VBO ($V_c \simeq 0.44$ eV), above which the HH becomes completely localized within ZnTe slabs. However, for VBO $\leqslant V_c$, the HH becomes confined at the hetero-interface. According to the best theoretical VBO determination, which is based on the state-of-the-art technique by Qteish *et al* [28], the VBO should decrease down to about 0.54 eV as the substrate's lattice constant ($a_{\parallel}$) increases. Thus, our results are in favour of an InAs substrate in order to achieve SLs of high optical quality. For this latter substrate, the VBO is the smallest possible, which yields a localization of the HH state at the interface and, therefore, an enhancement in the PL emissions.

From a fundamental research point of view, it seems that the common-cation II–VI heterostructures cannot be characterized by a vanishing CBO as has been speculated in the study of ZnS/ZnSe SLs [25, 26]. In contrast to these latter SLs, here in the present case of ZnSe/ZnTe SLs, the CBO is large and could be even of the same order as the VBO. Moreover, our results have also been compared to PL data and some conclusions have been drawn about the structural and optical qualities of the experimental samples. Finally, throughout our present investigation, we emphasize once more that the VBO values calculated by Qteish *et al* [29] for the studied SLs are found to be very reliable and give the best fit whenever coherent growth is achieved.

## Acknowledgments

The author would like to thank Professor M W C Dharma-wardana for his invitation to visit the NRC at Ottawa, where this investigation was started. His thanks are also extended to Professor A Hamza for a critical reading of the manuscript.

## References

[1] For a review, see for instance: Neumark G F, Park R M and DePuydt M 1994 *Phys. Today* **47** 26
[2] Cloitre T, Briot O, Gil B, Bertho D, Jancu J M, Ponga B E, Boring P, Mathieu H, Jouanin C and Aulombard R L 1993 *Physica* B **185** 109
[3] Takojima N, Ishizuka Y, Tsubono I, Kimura N, Suzuki K, Sawada T and Imai K 1996 *J. Cryst. Growth* **159** 489
[4] Faschinger W *et al* 1997 *Phys. Status Solidi* b **202** 695
[5] Rajakarunarayake Y, Miles R H, Wu G Y and McGill T C 1988 *Phys. Rev.* B **37** 10212
[6] Davies J J 1989 *Semicond. Sci. Technol.* **3** 219
[7] Lee D, Mysyrowicz A, Nurmikko A V and Fitzpatrick B J 1987 *Phys. Rev. Lett.* **58** 1475
[8] Yao T, Kato M, Davies J J and Tanino H 1988 *J. Cryst. Growth* **86** 552
[9] Chang S K, Lee C D, Park H L and Chung C H 1992 *J. Cryst. Growth* **117** 793
[10] Kobayashi M, Mino N, Kotagiri H, Kimura R, Konagai M and Takahashi K 1986 *Appl. Phys. Lett.* **48** 296

[11] Suntola T 1977 *US Patent*
[12] Konagai M, Kobayashi M, Kimura R and Takahashi K 1988 *J. Cryst. Growth* **86** 290
[13] Ozaki H, Imai K and Kumazaki K 1993 *J. Cryst. Growth* **127** 361
[14] Shen A, Xu L, Wang H, Chen Y and Wang Z 1993 *J. Cryst. Growth* **127** 383
[15] Yao T and Takeda T 1986 *Appl. Phys. Lett.* **48** 160
[16] Dosho S, Takemura Y, Konagai M and Takahashi K 1989 *J. Cryst. Growth* **95** 580
[17] Kuwabara H, Fujiyasu H, Aoki M and Yamada S 1986 *Japan. J. Appl. Phys.* **25** L707
[18] Yang H, Ishida A, Fujiyasu and Kuwabara H 1989 *J. Appl. Phys.* **65** 2838
[19] Nakashima S, Wada A, Fujiyasu H, Aoki M and Yang H 1987 *J. Appl. Phys.* **62** 2009
[20] Wu Y H, Yang H, Ishida A, Fujiyasu, Nakashima S and Tahara K 1989 *Appl. Phys. Lett.* **54** 239
[21] Baldereschi A, Baroni S and Resta R 1988 *Phys. Rev. Lett.* **61** 734
[22] Priester C, Bertho D and Jouanin C 1993 *Physica* B **191** 1
[23] Qteish A and Needs R J 1993 *Phys. Rev.* B **47** 3714
[24] Tit N and Al-Zarouni A 2002 *J. Phys.: Condens. Matter* **14** 7835
[25] Shazad K, Olego D J and Van de Walle C G 1988 *Phys. Rev.* B **38** 1417
[26] Tit N 2003 *J. Phys. D: Appl. Phys.* **36** 961
[27] Wu Y-H, Shizuo F and Shigeo F 1990 *J. Appl. Phys.* **67** 908
[28] Malonga F, Bertho D, Jouanin C and Jancu J M 1995 *Phys. Rev.* B **52** 5124
[29] Said R, Qteish A and Meskini N 1998 *J. Phys.: Condens. Matter* **10** 8703
[30] Slater J C and Koster G F 1954 *Phys. Rev.* **94** 1498
[31] Vögl P, Hjalmarson H P and Dow J D 1983 *J. Phys. Chem. Solids* **44** 365
[32] Kobayashi A, Sankey O F and Dow J D 1982 *Phys. Rev.* B **25** 6367
[33] Bertho D, Jancu J M and Jouanin C 1994 *Phys. Rev.* B **50** 16956
[34] Bertho D, Boiron D, Simon A and Jouanin C 1991 *Phys. Rev.* B **44** 6118
[35] Löwdin P O 1950 *Phys. Rev.* **18** 365
[36] Van de Walle C G 1989 *Phys. Rev.* B **39** 1871
[37] Tersoff J 1986 *Phys. Rev. Lett.* **56** 2755
[38] Cloitre T, Briot O, Gil B, Bertho D, Jancu J M, Ponga B E, Boring P, Mathieu H, Jouanin C and Aulombard R L 1993 *Physica* B **185** 109